

Analysis of the Arequipa, southern Peru, earthquake of 23 June 2001 by using GNSS data

Atınç Pırtı*, Mehmet Eren

Pırtı, A., Eren, M. 2025. Analysis of the Arequipa, southern Peru, earthquake of 23 June 2001 by using GNSS data. *Baltica* 38 (2), 174–181. Vilnius. ISSN 1648-858X.

Manuscript submitted 27 March 2025 / Accepted 27 November 2025 / Available online 15 December 2025

© Baltica 2025

Abstract. Peru is located above the damaging Peru–Chile Trench, which is the line where the Nazca Plate is subducting under the South American Plate. The two plates are approaching one another at a velocity of around 78 millimetres each year. There is a history of really big earthquakes in southwest Peru. The Arequipa, southern Peru, earthquake of 23 June 2001 had a moment magnitude of 8.4, a maximum Mercalli severity of VIII (severe), and occurred at 20:33:15 UTC (15:33:15 local time). It was the worst earthquake to ever strike the world since the 1965 Rat Islands earthquake and the most destructive earthquake to strike Peru since the disastrous Ancash earthquake of 1970. In this study, the horizontal and vertical displacements before and after the Arequipa, southern Peru, earthquake were analysed (kinematic GNSS results were compared with static GNSS results). As a result of these GNSS investigations (pre-motion on 20–21 June 2001), the obtained GNSS data for the precursor of the Arequipa earthquake were used. The AREQ IGS station before the earthquake, the movement in the horizontal components that occurred on 20–21 June 2001, and the decrease of this movement on 22 June 2001 seem to be a harbinger of the earthquake. In addition, the effects of the earthquake that occurred on 23 June 2001 were continued with aftershocks on 24 June 2001. In addition, this study may serve as a basis for understanding potential precursory patterns in this region.

Keywords: earthquake; Arequipa; Kinematic-Static GNSS; motion; precursor

Atınç Pırtı* (atinc@yildiz.edu.tr),  <http://orcid.org/0000-0001-9197-3411>; Mehmet Eren;

Department of Geomatic Engineering, Yıldız Technical University, 34220 Esenler, Istanbul, Türkiye

*Corresponding author

INTRODUCTION

Earthquakes are major natural disasters that cause destruction and loss of life. Precursor earthquakes are of great social and economic importance. The Nazca Plate is moving east-northeast relative to the South American Plate at an annual rate of about 78 mm/year. Plunging into the mantle along the Peru–Chile trench, the Nazca Plate can produce earthquakes at the depths of more than 600 km. This movement causes inter-plate thrust earthquakes at shallow depths (10–60 km). From the 20th century to the present day, several large earthquakes on the M8+ scale have occurred in this region. These include the 1960 Mw 9.5 Chile earthquake and the 2010 Mw 8.8 Chile earthquake (Métois *et al.* 2016; Argus *et al.* 2011). The June 23, 2001 Arequipa earthquake with a moment

magnitude (Mw) of 8.4 was studied in detail by the USGS (United States Geological Survey). This earthquake, with a maximum Mercalli intensity estimated as VIII (severe), caused major damage in the Tacna, Moquegua and Arequipa regions of southern Peru and was one of the most important seismic events in recent history (Giovanni *et al.* 2002; Curtis 2002; Hergert, Heidbach 2006; Philibosian 2024).

Surface deformations after the earthquake have created impacts such as cracks, landslides and collapse of drainage systems, and it is thought that such surface changes may have lasting impacts on ecosystems and landscapes in the long term (Keefer, Moseley 2004; Lavery *et al.* 2024; Kumar *et al.* 2016; Pritchard *et al.* 2007). Several studies have been conducted to understand the Arequipa earthquake, an important geological event. For example, Pichon *et al.*

(2002) analysed infrasonic waves and ground-related air waves detected after the Arequipa earthquake. The waves were found to propagate from northwest to southeast at a velocity of 3.3 km per second, providing valuable data on the earthquake's refraction dynamics and its impact on the acoustic signature in the atmosphere (Pichon *et al.* 2002). Ocola (2008) conducted a study to determine the geologic variations of co-seismic plunges from the Arequipa earthquake.

Bilek and Lay (2018) analysed the main shock and aftershocks in detail to determine the moment oscillation distributions and the pattern of aftershocks following the Arequipa earthquake. The study provides important evidence for the importance of aftershock behaviour in seismic hazard assessments, as the earthquake resulted in a significant rupture over an area of 180 km to the southeast, related to another seismic event in 1868 (Bilek, Ruff 2002). Naranjo and Clavero (2005) evaluated the impact of seismic events on geologic features in a study of unusual high flows triggered by the Arequipa earthquake. The study found that prolonged post-earthquake vibrations combined with a period of much above-normal rainfall in Bolivia caused high flows. This study highlights the complex relationships between seismic events and environmental conditions, providing important insights into how earthquake dynamics can trigger secondary geological phenomena (Naranjo, Clavero 2005). Devlin *et al.* (2012) analysed the stress changes that occur after large earthquakes and their effects on other earthquakes that follow. The study found that several earthquakes in the aftermath of the Arequipa earthquake occurred as a result of severely altered stress fields (Gutscher *et al.* 2000; Loverly *et al.* 2024; Bevis *et al.* 2001; Devlin *et al.* 2012; Jara *et al.* 2018). This study contributes to a better understanding of seismic hazards following large earthquakes. The main objective of this study is to analyse the movements before and after the Arequipa earthquake. By analysing the pre-earthquake motions, it is aimed to contribute to the precursor models. Furthermore, understanding the relationship between the Arequipa earthquake and large earthquakes that occurred in the historical period is critical for predicting future seismic events. In this situation, horizontal and vertical displacement analyses will be performed by using Global Navigation Satellite System (GNSS) data in the region, thus providing a scientific basis for risk reduction. In addition, the kinematic processing of GNSS measurements before, during and after the earthquake is planned. The kinematic processing of GNSS data is an important method to detect earthquakes in advance (Jara *et al.* 2018). This approach will contribute to the development of precursor and early warning systems for future earthquakes, especially by revealing potential indicators that can be used in the early detection

of seismic events. The objective of the study was to examine the secant features of the earthquake and the earthquake-related ground displacements. The findings show that the earthquake partially filled a seismic gap that has been recognized since 1868, making an important contribution to the understanding of seismic gaps and future seismic hazards (Ocola 2008; Dorbath *et al.* 1990; Hergert, Heidbach 2006; Philibosian 2024; Pritchard, Fielding 2008).

MATERIALS AND METHODS

Along the Peru–Chile Trench, Peru is located above the destructive border where the Nazca Plate is subducting under the South American Plate. Every year, the rate of convergence between the two plates is around 78 mm. Large-scale earthquakes have historically occurred in southwest Peru (Fig. 1). It appears that a portion of the plate boundary section that caused the magnitude 9.0 earthquake in 1868 was ruptured during the 23 June 2001 shock, which occurred roughly southeast of the source of the magnitude 7.7 earthquake in 1996. In communities that were severely destroyed by the 23 June 2001 earthquake, the 1868 earthquake had a devastating effect. The South American coast had hundreds of fatalities from the 1868 earthquake-caused tsunami, which also damaged Hawaii and resulted in the only known tsunami deaths in New Zealand (Gagnon *et al.* 2005; Perfettini *et al.* 2005; Shimazaki, Nakata 1980; Philibosian 2024).

As can be seen in Figs 1 and 2, the Arequipa earthquake that occurred on 23 June 2001 was the recurrence of earthquakes of 1604 (moment magnitude, Mw 8.8), 1784 (Mw 8.4) and 1868 (Mw 8.8). The recurrence period of these earthquakes in this region was approximately between 84 and 180 years. In general, these earthquakes differ in magnitude according to the width and length of the fault at the epicentre (Philibosian 2024; Li, Chen 2023; Fig. 2b).

RESULTS AND DISCUSSIONS

The knowledge of the tectonic processes involved in the Arequipa-Peru earthquake requires the understanding of the amount of displacement brought about by the earthquake. In this circumstance, the data of AREQ station (IGS GNSS station) close to the earthquake epicentre is quite helpful. In this study, the data of the AREQ station on the IGS network that are close to the epicentre of the Arequipa-Peru earthquake were collected and analysed (see Figs 1 and 2, Table 1). The AREQ points' coordinates and standard deviations are shown in Table 1. The displacements due to the earthquake were determined by analysing the time series obtained from the daily (19–24 June

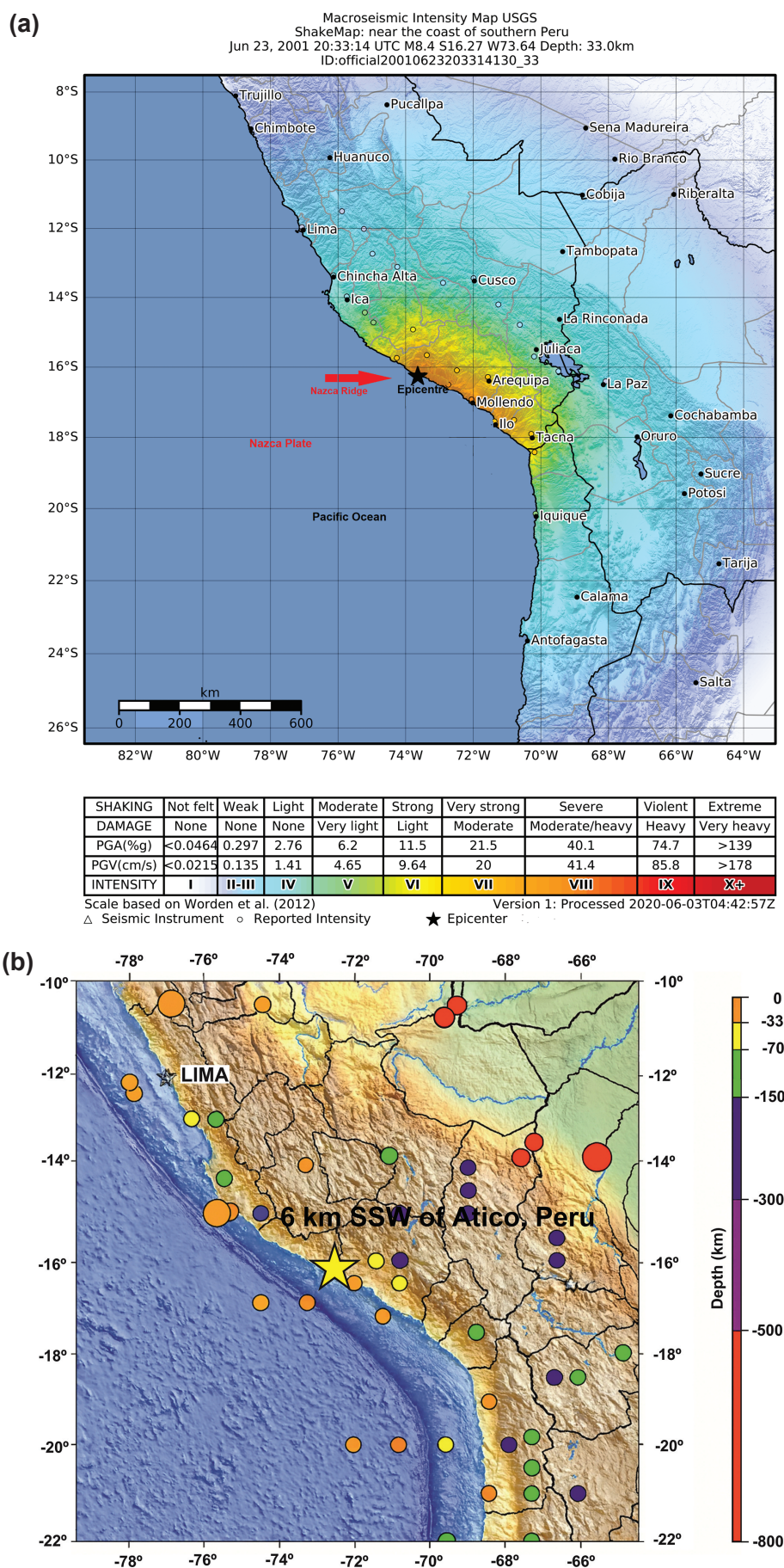
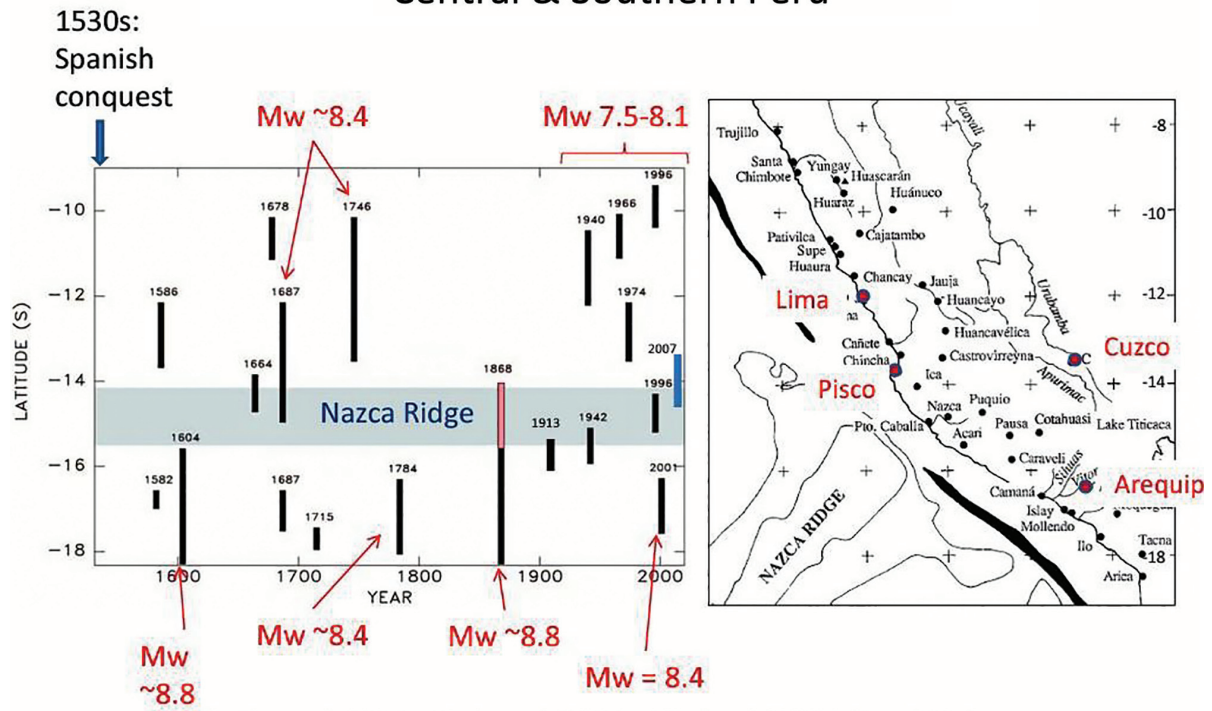


Fig. 1 (a) Main event, epicentre marked with a star (USGS 2001, modified) and (b) aftershock locations through 23 June 2001 (Pararas-Carayannis 1965, 1968, 1969, 1974, 1972, 1977 and 2012, modified)

(A)

Central & Southern Peru



(B)

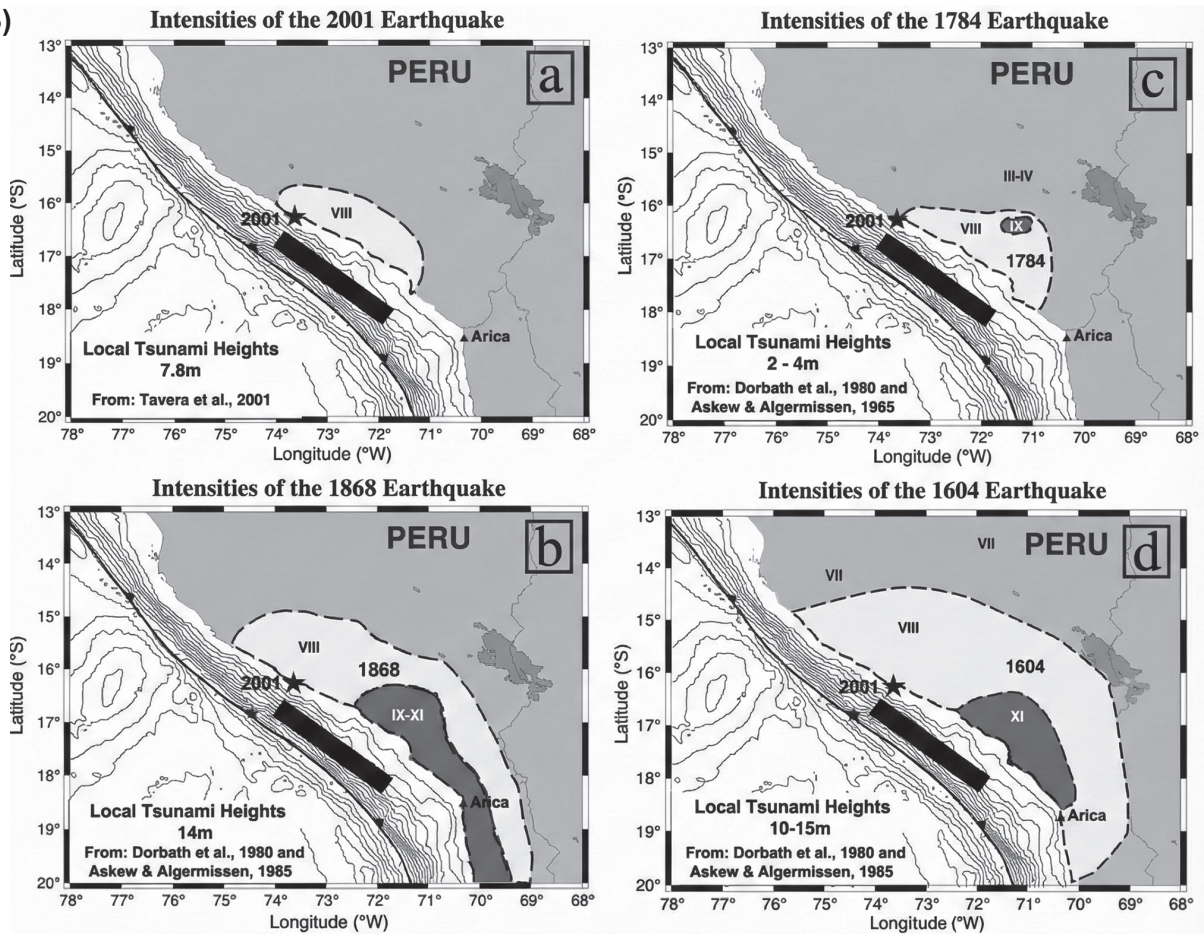


Fig. 2 (A) The earthquake graphic of central and southern Peru; after Philibosian 2024. (B) Earthquakes intensity in Arequipa, Peru; after Pritchard *et al.* 2007, Pritchard *et al.* 2008, Hayes *et al.* 2016, Lavery *et al.* 2024 (a-d)

2001) GNSS data solutions (Figs 3, 4 and 5). As noted in the preceding part, the data of the AREQ station from the IGS network were processed by kinematic and static GNSS methods. On 19–24 June 2022, the GNSS data were analysed to study the earthquake impacts seen in the time series (00:00:00–23:59:30 UTC Time). From the IGS network servers, 24 hours' duration RINEX observation data with a thirty-second interval were downloaded during this time period. Using CSRS-PPP Software to process by static (30 sec interval) and kinematic methods (00:00:00–23:59:30 UTC Time 30 sec interval), the 24-hour RINEX observation files (19–24 June 2001) of the AREQ station were analysed. Static and kinematic processing results were obtained by using CSRS-PPP Software (24 hours). During the monitoring period (19 June 2001), the standard deviations of coordinates were computed with an accuracy of 6–13 mm in the horizontal components and 30 mm in the vertical components.

The effect of the Arequipa, Peru, earthquake on the AREQ IGS point is shown in Fig. 3. It seems that the motion of the AREQ point is in the north and south directions before the earthquake (20–21 June 2001), as seen in Fig. 3. The effect of the Arequipa-Peru earthquake on the AREQ point is shown in Fig. 3e. It seems that the motion of the AREQ point is in the north-west and south-east directions during the earthquake (Fig. 3). It is obvious that the earthquake

significantly affected the horizontal coordinate data (Fig. 4). Based on the time series of coordinate differences from the AREQ station, the horizontal coordinates changed by about 1–10 cm and the height coordinates changed by about 10–45 cm by using the three-dimensional displacement components of the AREQ point computed by using GNSS data, as illustrated in Fig. 4.

The two-dimensional vectorial motions of the AREQ station on 19, 20, 21, 22, 23 and 24 June 2001 are shown in Fig. 3. The vectorial motions on 20 and 21 June differed from the other days. On 20 June, the motions were north and south (Fig. 3b), while on 21 June, the motions were south, south-east and south-west (Fig. 3c). The earthquake occurred on 23 June 2001, at 20:33:15 UTC Time. On 22 June, a decrease in the motions was observed. On 23 June, GNSS data could not be recorded for a certain period of time due to a lot of problems that occurred during the earthquake. Towards the end of the day, GNSS data could be recorded again, and the obtained GNSS data were processed. The initial movement of the AREQ station due to the earthquake was in the north-west and south-east direction (Fig. 3e).

On 24 June 2001, the effect of the earthquake of 23 June 2001 (Mw 8.4) continued with Mw 7.9 and the south-west movement reached 50 cm (Fig. 4). It is obvious that the horizontal motion of the earthquake of 23 June 2001 (1.25 m) decreased to 0.50 m

Table 1 Standard deviation, coordinate (ITRF05, Epoch 2001.5) values of the two stations by using the static method

Name	Latitude (°)	Longitude (°)	h (m)	Std lat (m)	Std lon (m)	Std h (m)
AREQ	-16°27' 55.84953"	-71°29' 34.04942"	2488.926	0.006	0.013	0.030

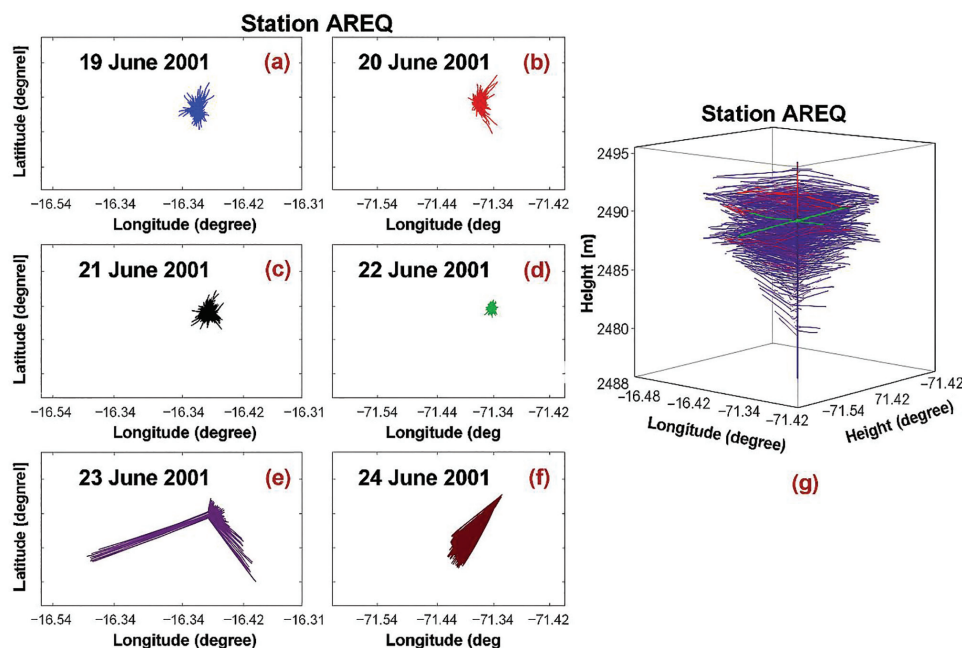


Fig. 3 Earthquake-induced horizontal displacement vectors of AREQ point on 19, 20, 21, 22, 23 and 24 June 2001

and then continued with this value as a result of the aftershocks (Mw 7.9) on 24 June 2001. Figure 3g shows the three-dimensional coordinate differences (kinematic-static) obtained from the earthquakes at the AREQ station. On 23 June, there was a swell motion, and on 24 June, there was a collapse motion. The swell motion was computed to be approximately 0.75 m, while the collapse motion was calculated to be 0.50 m (Fig. 4).

A large earthquake of 23 June 2001 occurred off the coast of Peru, close to a little Hacienda La Federal hamlet. At a distance of 120 miles (190 km), the 8.1-magnitude earthquake brought down ancient structures in Arequipa. The earthquake occurred at the intersection of the South American and Nazca tectonic plates, 20 miles (33 km) below the surface. The Andes Mountains are rising, and volcanism is occur-

ring as a result of the Nazca Plate being forced under (subducted by) the South American Plate.

Several months before the earthquake (on 15 December 2000) an image of the earthquake was captured by NASA's Terra satellite using the Advanced Space-borne Thermal Emission and Reflection Radiometer (ASTER) (Fig. 5a). Presented as red, green, and blue, the picture is really a fake colour composite made up of near-infrared, red, and green light. The foliage has a vivid crimson appearance (NASA 2024; Abrams *et al.* 2015; Fig. 5a).

In terms of geology, the image's deep stream valleys and coastal cliffs that stretch from top to bottom (north to south) show how quickly the ground is rising (Fig. 5b; Abrams *et al.* 2015; NASA 2024. The results of this study confirm the understanding that GNSS stations to be installed near the fault zone can be used for the earthquake precursor with artificial intelligence (in its broadest sense, it is intelligence exhibited by machines, machine learning, especially for computer systems) by using them continuously and evaluating the movements of the earthquakes in the region.

CONCLUSION

Large megathrust earthquakes along the subduction zone, such as the Arequipa earthquake in 2001 with a magnitude of 8.4, which caused considerable destruction, are a particular feature. The 23 June 2001 earthquake in Peru and its effects are analysed in this article. The earthquakes in Arequipa region of Peru recur at the intervals of 84 to 180 years. As a result of the investigations of the AREQ station before the 23 June 2001 earthquake, the movement in the horizontal components that occurred on 20–21 June 2001 and the decrease of this movement on 22 June 2001 seem to be a harbinger of the earthquake. In addition, the effects of the earthquake that occurred on 23 June 2001

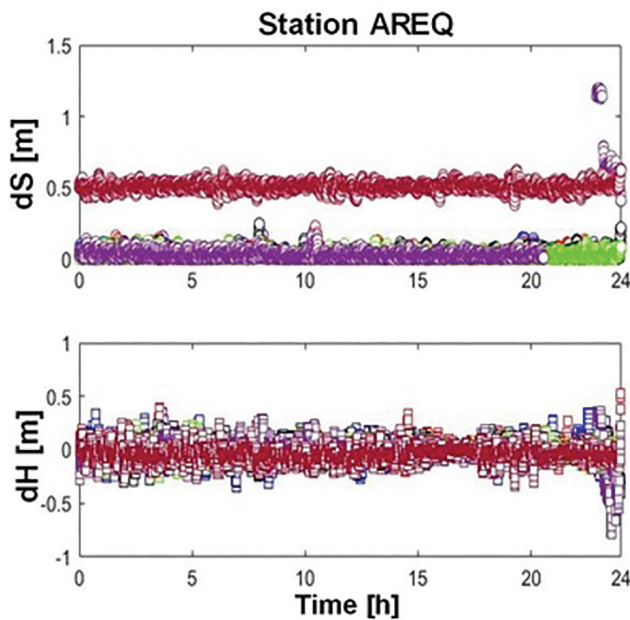


Fig. 4 Values of horizontal distances and height differences of the AREQ point between 19 and 24 June 2001

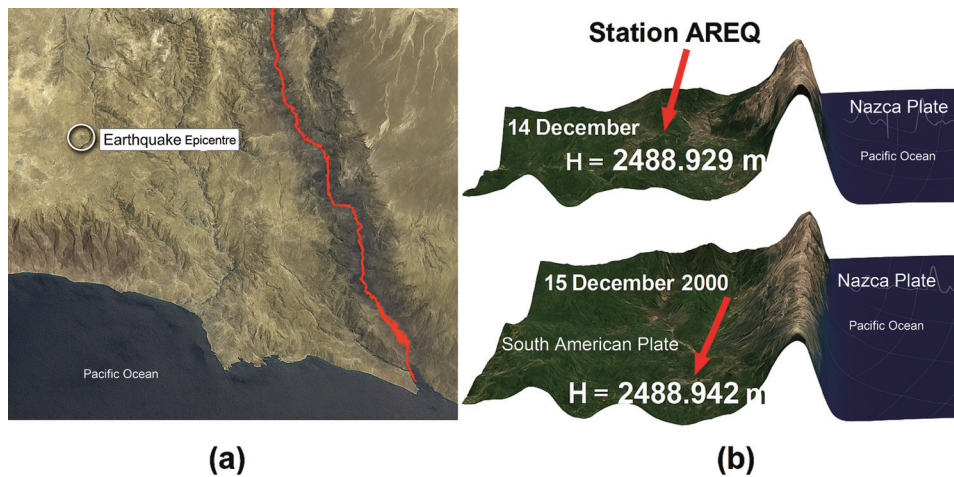


Fig. 5 (a) Arequipa earthquake epicentre on the ASTER aboard NASA's Terra spacecraft image. (b) Vertical deformation of the AREQ point and the surrounding region (after NASA 2024)

were continued with aftershocks on 24 June 2001. The movement in the horizontal component continued at 50 cm on 24 June 2001. This earthquake in 2001 and the horizontal movement that occurred before it can be used as a precursor for the earthquakes that will occur in this region in the future.

ACKNOWLEDGMENTS

The authors would like to thank the reviewer and the editorial board members for their valuable comments on the article.

REFERENCES

- Abrams, M., Tsu, H., Hulley, G., Iwao, K., Pieri, D., Cudahy, T., Kargel, J. 2015. The Advanced Spaceborne Thermal Emission and Reflection Radiometer (ASTER) after fifteen years: Review of global products. *International Journal of Applied Earth Observation and Geo-information* 38, 292–301. <https://doi.org/10.1016/j.jag.2015.01.013>
- Argus, D.F., Gordon, R.G., DeMets, C. 2011. Geologically current motion of 56 plates relative to the no-net-rotation reference frame, *Geochemistry, Geophysics, Geosystems* 12, Q11001. <https://doi.org/10.1029/2011GC003751>
- Bevis, M., Kendrick, E., Smalley Jr, R., Brooks, B., Allmendinger, R., Isacks, B. 2001. On the strength of interplate coupling and the rate of back arc convergence in the central Andes: An analysis of the interseismic velocity field. *Geochemistry, Geophysics, Geosystems* 2(11). <https://doi.org/10.1029/2001GC000198>
- Bilek, S., Ruff, L. 2002. Analysis of the 23 June 2001 $M_w = 8.4$ Peru underthrusting earthquake and its aftershocks. *Geophysical Research Letters* 29(20). <https://doi.org/10.1029/2002gl015543>
- Bilek, S.L., Lay, T. 2018. Subduction zone megathrust earthquakes. *Geosphere* 14(4), 1468–1500. <https://doi.org/10.1130/GES01608.1>
- Curtis L.E. (ed.) 2002. *Atico, Peru Mw 8.4 Earthquake of June 23, 2001*. Reston, VA: ASCE, TCLEE. ISBN 9780784406618
- Devlin, S., Isacks, B., Pritchard, M., Barnhart, W., Lohman, R. 2012. Depths and focal mechanisms of crustal earthquakes in the central Andes determined from teleseismic waveform analysis and INSAR. *Tectonics* 31(2). <https://doi.org/10.1029/2011tc002914>
- Dorbath, L., Cisternas, A., Dorbath, C. 1990. Assessment of the size of large and great historical earthquakes in Peru. *Bulletin of the Seismological Society of America* 80, 551–576.
- Gagnon, K., Chadwell, C.D., Norabuena, E. 2005. Measuring the onset of locking in the Peru–Chile trench with GPS and acoustic measurements. *Nature* 434(7030), 205–208. <https://doi.org/10.1038/nature03412>
- Giovanni, M.K., Beck, S.L., Wagner, L. 2002. The June 23, 2001 Peru earthquake and the southern Peru subduction zone. *Geophysical Research Letters* 29(21). <https://doi.org/10.1029/2002GL015774>
- Gutscher, M.A., Spakman, W., Bijwaard, H., Engdahl, E.R. 2000. Geodynamics of flat subduction: Seismicity and tomographic constraints from the Andean margin. *Tectonics* 19(5), 814–833. <https://doi.org/10.1029/1999TC001152>
- Hayes, G.P., Meyers, E.K., Dewey, J.W., Briggs, R.W., Earle, P.S., Benz, H.M., Smoczyk, G.M., Flamme, H.E., Barnhart, W.D., Gold, R.D., Furlong, K.P. 2016. Tectonic summaries of magnitude 7 and greater earthquakes from 2000 to 2015. *USGS Open-File Report 2016*, 1192.
- Hergert, T., Heidbach, O. 2006. New insights into the mechanism of post-seismic stress relaxation exemplified by the 23 June 2001 $M_w = 8.4$ earthquake in southern Peru. *Geophysical Research Letters* 33(2), L02307. <https://doi.org/10.1029/2005GL024858>
- Jara, J., Sánchez-Reyes, H., Socquet, A., Cotton, F., Virieux, J., Maksymowicz, A. 2018. Kinematic study of Iquique 2014 $M_w 8.1$ earthquake: Understanding the segmentation of the seismogenic zone. *Earth and Planetary Science Letters* 503, 131–143. <https://doi.org/10.1016/j.epsl.2018.09.025>
- Keefer, D.K., Moseley, M.E. 2004. Southern Peru desert shattered by the great 2001 earthquake: Implications for paleo-seismic and paleo-El Niño–Southern Oscillation records. *Proceedings of the National Academy of Sciences* 101(30), 10878–10883.
- Kumar, V., Kumar, D., Chopra, S. 2016. Estimation of source parameters and scaling relations for moderate size earthquakes in North-West Himalaya. *Journal of Asian Earth Sciences* 128, 79–89.
- Li, S., Chen, L. 2023. How long can the post-seismic and interseismic phases of great subduction earthquake sustain? Toward an integrated earthquake-cycle perspective. *Geophysical Research Letters* 50(11), e2023GL103976. <https://doi.org/10.1029/2023GL103976>
- Loverly, B., Chlieh, M., Norabuena, E., Villegas-Lanza, J.C., Radiguet, M., Cotte, N., et al. 2024. Heterogeneous locking and earthquake potential on the South Peru megathrust from dense GNSS network. *Journal of Geophysical Research: Solid Earth* 129, e2023JB027114. <https://doi.org/10.1029/2023JB027114>
- Metois, M., Vigny, C., Socquet, A. 2016. Interseismic coupling megathrust earthquakes and seismic swarms along the Chilean subduction zone (38°–18°S). *Pure and Applied Geophysics* 173(5), 1431–1449. <https://doi.org/10.1007/s00024-016-1280-5>
- Naranjo, J., Clavero, J. 2005. A rare case of grass flow induced by the Mw 8.4 Arequipa earthquake, June 2001, in the Altiplano of northern Chile. *Quaternary Research* 64(2), 242–248. <https://doi.org/10.1016/j.yqres.2005.06.004>
- Ocola, L. 2008. Southern Peru co-seismic subsidence: 23 June 2001, 8.4-Mw earthquake. *Advances in Geosciences* 14, 79–83. <https://doi.org/10.5194/adgeo-14-79-2008>

- Pararas-Carayannis, G. 1968. The Tsunami of October 17, 1966 in Peru. *International Tsunami Information Center Newsletter 1*(1), March 5. <https://www.drgeorgepc.com/Tsunami1966Peru.html>
- Pararas-Carayannis, G. 1969. Catalog of Tsunami in the Hawaiian Islands. *World Data Center A- Tsunami*. U.S. Department of Commerce Environmental Science Service Administration Coast and Geodetic Survey, May 1969, 94 pp.
- Pararas-Carayannis, G. 1972. The Great Alaska Earthquake of 1964 Source Mechanism of the Water Waves Produced. In: *National Academy of Sciences – Committee on the Alaska Earthquake, Volume on Seismology and Geodesy*, 249–258.
- Pararas-Carayannis, G. 1974. An Investigation of Tsunami Source Mechanism off the Coast of Central Peru. *Marine Geology 17*(4), 235–247. [https://doi.org/10.1016/0025-3227\(74\)90074-7](https://doi.org/10.1016/0025-3227(74)90074-7)
- Pararas-Carayannis, G. 2012. Geodynamics of Nazca Ridge's oblique subduction and migration – Implications for tsunami generation along Central and Southern Peru: Earthquake and tsunami of 23 June 2001. *Science of Tsunami Hazards 31*, 129–153.
- Pararas-Carayannis, G., Augustine, S.F. 1965. *Source Mechanism Study of the Alaska Earthquake and Tsunami of 27 March 1964*. Part I, Water Waves, edited by George Pararas-Carayannis; Part II, *Analysis of Raleigh Wave*, edited by Augustine Furumoto. *Report HIG65-17*, 42 pp. Honolulu: Hawaii Institute of Geophysics, December 1965.
- Pararas-Carayannis, G., Calebaugh, P.J. 1977. Catalog of Tsunamis in Hawaii, Revised and Updated. In: *World Data Center A for Solid Earth Geophysics*, NOAA, 78 pp., March 1977.
- Perfettini, H., Avouac, J.-P., Ruegg, J.C. 2005. Geodetic displacements and aftershocks following the 2001 $M_w = 8.4$ Peru earthquake: Implications for the mechanics of the earthquake cycle along subduction zones. *Journal of Geophysical Research 110*(B9), B09404. <https://doi.org/10.1029/2004JB003522>
- Pichon, A., Guilbert, J., Vega, Á., Garcés, M., Brachet, N. 2002. Ground-coupled air waves and diffracted infrasound from the Arequipa earthquake of June 23, 2001. *Geophysical Research Letters 29*(18). <https://doi.org/10.1029/2002gl015052>
- Pritchard, M.E., Fielding E.J. 2008. A study of the 2006 and 2007 earthquake sequence of Pisco, Peru, with InSAR and teleseismic data. *Geophysical Research Letters 35*(9). <https://doi.org/10.1029/2008GL033374>
- Pritchard, M.E., Norabuena, E.O., Ji, C., Boroschek, R., Comte, D., Simons, M., et al. 2007. Geodetic, teleseismic, and strong motion constraints on slip from recent southern Peru subduction zone earthquakes. *Journal of Geophysical Research 112*(B3), B03307. <https://doi.org/10.1029/2006JB004294>
- Shimazaki, K., Nakata, T. 1980. Time-predictable recurrence model for large earthquakes. *Geophysical Research Letters 7*, 279–282. <https://doi.org/10.1029/GL007i004p00279>

Internet sources

- NASA 2024. *The Advanced Space-borne Thermal Emission and Reflection Radiometer*. <https://asterweb.jpl.nasa.gov/>
- Philibosian, B. 2024. *Great Earthquakes of Peru*. https://www.google.com/url?sa=i&url=https%3A%2F%2Fweb.gps.caltech.edu%2F~clay%2FPeruTrip%2FTalks%2FPhilibosian_PeruEQs.pdf&psig=AOvVaw2HfZeYDALvOLTHkyfSfzqW&ust=1717509407543000&source=images&cd=vfe&opi=89978449&ved=0CAcQrpoMahcKEwiYx-H7y7-GAxUAAAAAHQAAAAAQBA
- USGS 2021. Mw 8.4-6 km SSW of Atico, Peru, https://earthquake.usgs.gov/earthquakes/eventpage/official20010623203314130_33/executive